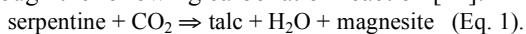


**SPECTRAL EVIDENCE FOR THE CARBONATION OF SERPENTINE IN NILI FOSSAE, MARS.** C. E. Viviano, J. E. Moersch, and H. Y. McSween, University of Tennessee, Department of Earth & Planetary Sciences (cviviano@utk.edu).

**Introduction:** Recently, alteration phases including Fe/Mg-phyllsilicates, zeolites, prehnite, chlorite, serpentine, illite (or muscovite), kaolinite, and hydrated silica have been identified in the Nili Fossae region of Mars (Fig. 1) [1-3]. These minerals, identified from high spatial and spectral resolution CRISM data, are interpreted to be products of low-grade thermal metamorphism and hydrothermal interaction, along with diagenesis, suggesting that past aqueous alteration of the crust occurred at elevated temperatures [2], [4].

Serpentine-bearing rocks in the Nili Fossae region are indicative of hydrothermal alteration of ultramafic rocks [5] and are found in association with an olivine-rich [6-9] draping unit that overlies a unit containing Mg-smectite, a stratigraphic relationship found throughout the Nili Fossae region [10]. The spectral signature of magnesium carbonate, first identified by [11], is also associated with the underlying Mg-smectite and has been hypothesized to be a weathering product of either the olivine or serpentine in this region [2],[3],[12]. [11] suggested a potential formation mechanism for the carbonate-bearing unit, in which impact or volcanic heating of the olivine-bearing material led to hydrothermal alteration along the contact with the underlying water-bearing Mg-smectite unit. It has also been suggested that the Mg-smectite phase could actually be talc based on the assertion that the two phases are spectrally indistinguishable [12]. The consequence of this new spectral interpretation was a modified hydrothermal hypothesis, in which the phyllosilicate was formed at the same time as the overlying carbonate-bearing unit by a single hydrothermal event through the following carbonation reaction [12]:



If correct, this hypothesis suggests that the phyllosilicate and carbonate-bearing units are simply the result of different temperatures regimes within the zone of hydrothermal alteration [12]. The purpose of this work is to further test this hypothesis by characterizing and identifying spectral features of those Fe/Mg phyllosilicates associated with the ultramafic terrain in the Nili Fossae region. Their composition has important implications for the geologic history of this region, and its presence may help constrain pressure and temperature regimes present during its formation as well as the geologic history of the region.

**Methods:** The CRISM BD2290 and D2300 [13] spectral parameters were used to map Fe/Mg smectites. Also, two spectral parameters from [14] that indicate

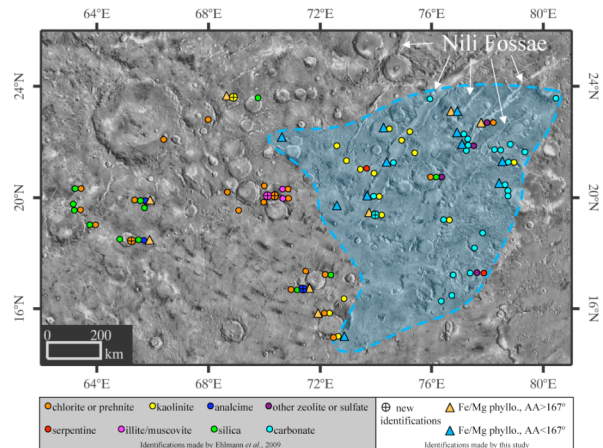


**Figure 1.** Nili Fossae region with locations of alteration minerals identified by [5] (open circles) and by this study (circles with cross hairs). Orange triangles indicate a detection of Fe/Mg phyllosilicates associated with chloritization; blue triangles indicate a detection of Fe/Mg phyllosilicates associated with talc (this study).

the degree of smectite chloritization were calculated for spectra from areas identified as containing Fe/Mg phyllosilicates. Figure 2 shows laboratory spectra of saponite and talc. Both phases share similar indistinguishable absorption features with similar relative band depths (compared to the local continuum) at 2.31 and 2.39  $\mu\text{m}$ . However, the gap between the local continuum and the septum at 2.35  $\mu\text{m}$  (between the two absorption bands) is greater in the talc spectrum than the saponite spectrum, and is a consistent difference throughout a suite of spectra of both phases. The magnitude of the continuum-septum gap is given by the relative band depth between the local continuum defined at  $\sim 2.2$  and 2.42  $\mu\text{m}$  and the local maximum of the septum at 2.35  $\mu\text{m}$ . To distinguish between talc and other phyllosilicate phases (e.g., chlorite) that also display reflectances at 2.35  $\mu\text{m}$  below the local continuum, a second spectral parameter is necessary. These phases have an additional absorption feature at 2.210  $\mu\text{m}$ , which talc lacks. Thus, a plot of relative band depth at 2.355  $\mu\text{m}$  versus relative band depth at 2.210  $\mu\text{m}$  (Fig. 3) provides a means to distinguish between

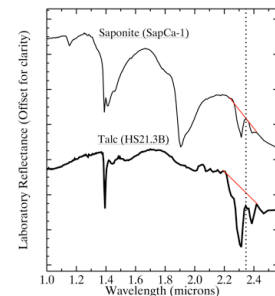


**Figure 2.** Comparison of saponite vs. talc laboratory spectra. A larger gap between the local continuum (red) and the septum at 2.35  $\mu\text{m}$  (dotted black vertical line) is present in only the talc spectrum. Library spectra from [15].

by the relative band depth between the local continuum defined at  $\sim 2.2$  and 2.42  $\mu\text{m}$  and the local maximum of the septum at 2.35  $\mu\text{m}$ . To distinguish between talc and other phyllosilicate phases (e.g., chlorite) that also display reflectances at 2.35  $\mu\text{m}$  below the local continuum, a second spectral parameter is necessary. These phases have an additional absorption feature at 2.210  $\mu\text{m}$ , which talc lacks. Thus, a plot of relative band depth at 2.355  $\mu\text{m}$  versus relative band depth at 2.210  $\mu\text{m}$  (Fig. 3) provides a means to distinguish between

talc, prehnite/chlorite, and other Fe/Mg phyllosilicates spectrally.

**Results and Discussion:** In Figure 3, Nili Fossae Fe/Mg phyllosilicate spectra are plotted using the

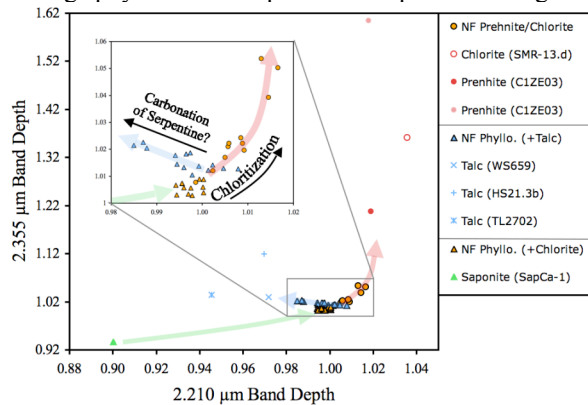


**Figure 3.** Continuum-removed band depth at 2.35  $\mu\text{m}$  versus 2.210  $\mu\text{m}$  for Fe/Mg smectite and chlorite phases in the Nili Fossae (NF) region (outlined symbols). Library spectra from [15] and RELAB.

aforementioned parameters. Those consistent with chloritization (orange triangles), as inferred from parameters by [14], fall along a trend between a laboratory smectite (saponite) and chlorite on this plot. Those that appear to diverge from these points (blue triangles) trend towards laboratory spectra of talc, and occupy region of the plot distinct from smectite or chlorite. Interestingly, the phyllosilicates that trend towards talc appear to originate in a region partway along the trend between smectite and chlorite. This suggests that, as chloritization increased through continued burial, carbonation occurred after burial to a particular depth.

A map of Fe/Mg phyllosilicates associated with chloritization and the presence of talc (Fig. 1) shows that the two populations occupy geographically distinct regions surrounding the Nili Fossae (blue dashed region). Talc-related phyllosilicates are found in the olivine-rich eastern portion of the region, whereas the chlorite-related phyllosilicates are found mostly, but not exclusively, in the western portion of the region. Wherever carbonate has been identified (blue circles), only the talc-related phyllosilicate is observed. Chlorite-related phyllosilicates are dominantly associated with occurrences of prehnite/chlorite phases (orange circles). There are some locations that possess both types of phyllosilicates.

Talc-related phyllosilicate originating from a localized point along the carbonation trend (Fig. 3) suggests that the  $\sim 800$  square km area in eastern part of the region experienced a relatively uniform depth of burial. This is also the portion of the Nili Fossae region where the olivine-rich cap unit and underlying magnesite are found, as well as the two documented occurrences of

serpentine in the region. The local geographic association of serpentine, magnesite, and potentially talc provides the necessary solid reactants and products for the serpentinization and carbonation processes described in equation 1.

Evidence for the carbonation reactions appears throughout this  $\sim 800$  square km area, though it could not have run to completion across the entire region because serpentine is still observed. Complete carbonation of serpentine is achieved with low fluid to rock ratios at temperatures  $\leq 200^\circ\text{C}$ , but if temperatures remain this low, extended fluid interaction at low temperatures can result in the decarbonation and silicification of the altered rock [16]. If temperatures increase above  $200^\circ\text{C}$ , even high levels of fluid interaction will not cause the dissolution of carbonate [16]. Because the magnesium carbonate in the Nili Fossae region persists, either the temperature of the ultramafic protolith remained low and fluid interactions were limited, or temperatures reached above  $200^\circ\text{C}$ .

**Conclusions:** We put forth the following possible sequence of events for the development of alteration assemblages and stratigraphic relationships found in the easternmost portion of the region: 1) alteration of Noachian-aged crust to Fe/Mg smectite, 2) uniform burial and chloritization of this material by Hesperian lava flows, 3) hydrothermal alteration and serpentinization of ultramafic protolith (lava flows), 4) carbonation of serpentine to form magnesium carbonate and talc-bearing material mixed with the underlying Noachian mixed-layer clay during a single hydrothermal event as hypothesized by [12]. Further characterization of Fe/Mg phyllosilicates in this region and other olivine-rich lithologies on Mars may indicate carbonation of serpentine was a widespread process on Mars and is the reason for the limited occurrence of serpentine [5]. If carbonation of serpentine was a global process, this reaction could provide an atmospheric sink for  $\text{CO}_2$  and may have been a significant part of the Martian carbon cycle in the past.

**References:** [1] Mustard et al. (2008) *Nature*, 454, 305-309. [2] Ehlmann et al. (2009) *JGR*, 114, E00D08. [3] Ehlmann et al. (2011) *Clays Clay Miner.*, 59, 359-377. [4] Ehlmann et al. (2010) *GRL*, 37, L06201. [5] Ehlmann et al. (2009) *JGR*, 114, E00D08. [6] Hoefen et al. (2003) *Science*, 302. [7] Mustard et al. (2005) *Science*, 307. [8] Hamilton & Christensen, 433-436. (2005) *Geology*, 33. [9] Koepfen and Hamilton (2008) *JGR*, 113. [10] Mangold et al. (2007) *JGR*, 112, E08S04. [11] Ehlmann et al. (2008) *Science*, 322, 1823-1831. [12] Brown et al. (2010) *Earth Plan. Sci. Let.*, 297, 174-182. [13] Pelkey et al (2007) *JGR*, 112, E08S14. [14] Milliken et al. (2010) *LPSC XLII*, #2030. [15] Clark et al (2007) *USGS*, 231. [16] Klein and Garrido (2011) *Lithos*, 126, 147-160.